Mechanism of Membrane Permeabilization by Sticholysin I, a Cytolysin Isolated from the Venom of the Sea Anemone *Stichodactyla helianthus*[†]

Mayra Tejuca,[‡,§] Mauro Dalla Serra,[‡] Mercedes Ferreras,[‡] Maria E. Lanio,[§] and Gianfranco Menestrina*,[‡]

*Centro di Fisica degli Stati Aggregati, Consiglio Nazionale delle Ricerche−Istituto Trentino di Cultura,
I-38050 Povo (Trento), Italy, and Departamento de Bioquimica, Facultad de Biologia, Universidad de la Habana,
La Habana, Cuba*

ABSTRACT: Actinaria cytolysins are very potent basic toxins isolated from the venom of sea anemones, which are supposed to exert their toxic activity through formation of oligomeric pores in the host plasma membrane. To gain insight into their mechanism of action, the interaction of *Stichodactyla helianthus* sticholysin I (St-I) with lipid bilayers was studied. St-I increased the permeability of calcein-loaded lipid vesicles composed of different phospholipids. The rate of permeabilization improved when sphingomyelin (SM) was introduced into phosphatidylcholine (PC) vesicles, reaching an optimum value at equimolar concentrations of these two phospholipids. It was also a function of the pH, showing a local maximum of activity between pH 8 and 9 and a marked decrease at pH 10 and 11. Under optimal conditions (e.g., PC:SM 1:1, pH 8, toxin to vesicle ratio < 200), most of the toxin is bound to the lipid phase. The reduced toxin effect at low and high SM content, or at high pH, is principally due to a decreased toxin binding. From the dose dependence of the permeabilization, at constant lipid concentration, it was inferred that St-I increases membrane permeability by forming oligomeric pores comprising at least three cytolysin monomers. The involvement of oligomers was also suggested by the dependence of calcein release on the vesicle concentration at constant toxin dose. In fact, the time course of dye release was well described under all circumstances by a kinetic model which assumes that trimerization leads to a conductive pore. All the relevant equilibrium and rate constants were derived. Addition of St-I to one side of a planar lipid membrane increased the conductivity of the film in discrete steps of defined amplitude, indicating the formation of ion channels. The dose dependence of this effect was the same as with LUV. The channel was cation-selective and its conductance suggested a functional radius of about 1.0 nm, consistent with the size of the lesion previously observed in red blood cells. Pores exhibited rectification and voltage-dependent gating.

Potent cytolysins have been extracted from the venom of at least 16 species of sea anemones [for recent reviews see Kem (1988), Bernheimer (1990), Harvey (1990), Turk (1991), and Macek (1992)]. Many such toxins (at least 27) have been isolated and characterized. They share a number of common properties: they are basic proteins, with pI between 8 and 12; they comprise a single polypeptide chain of molecular mass ranging from 16 to 20 kDa; they contain no cysteines or cystines; and they are strongly inhibited by sphingomyelin. A few of them have been sequenced (Blumenthal & Kem, 1983; Simpson et al., 1990; Mebs et al., 1992; Belmonte et al., 1994). At subnanomolar concentrations they cause erythrocyte lysis by opening pores, which are probably oligomeric. With some of them, the formation of discrete channels permeable to small ions and solutes has been demonstrated also in model lipid membranes (Michaels, 1979; Varanda & Finkelstein, 1980; Chanturya et al., 1990; Zorec et al., 1990; Belmonte et al., 1993). For

their common ability to form pores in lipid membranes they have received the family name of actinoporins (Kem, 1988).

Due to their extraordinary potency and chemical stability, these toxins can be used to construct chimeric molecules targeted at killing tumor cells (Avila et al., 1989; Pederzolli et al., 1995).

The sea anemone *Stichodactyla helianthus*, widely diffused in the Caribbean area, produces a venom that contains several active proteinaceous factors, among which are a neurotoxin acting on potassium channels (Castañeda et al., 1995), a protease inhibitor (Delfin et al., 1994), a phospholipase (Pazos et al., 1996), and at least two cytolysins belonging to the above-mentioned group (Alvarez et al., 1994, 1996). The isolation, purification to homogeneity, and primary sequence of one of these cytolysins, designated sticholysin I, has been described recently (Alvarez et al., 1996). This toxin is similar to the cytolysin C III[1] described earlier (Blumenthal & Kem, 1983); however, it contains a 22-residue

---

[1] Abbreviations: C III, *Stichodactyla helianthus* cytolysin III; St-I, *Stichodactyla helianthus* sticholysin I; EqT-II, *Actinia equina* equinatoxin II; BSA, bovine serum albumin; SM, sphingomyelin; PC, phosphatidylcholine; PE, phosphatidylethanolamine; POPC, palmitoyloleoylphosphatidylcholine; SUV, small unilamellar vesicles; LUV, large unilamellar vesicles; PLM, planar lipid membranes; TLC, thin-layer chromatography; SDS, sodium dodecyl sulfate; Triton X-100, octylphenoxy(polyethoxy)ethanol; PAGE, polyacrylamide gel electrophoresis; RBC, red blood cells.

inset which was missing in C III but is present in other parent cytolysins (Simpson et al., 1990; Mebs et al., 1992; Belmonte et al., 1994). It causes hemolysis by colloid osmotic shock and, using osmotic protectants, it was found that it forms a channel of ≈1-nm radius, whose size is constant over a wide range of toxin concentrations (Alvarez et al., 1996).

Sea anemone cytolysins are interesting examples of membrane-damaging toxins and their study could help understanding the action of this wide class of toxins and, more generally, the interaction of proteins with lipid membranes.

To elucidate the molecular mechanism of pore formation by sticholysin I we have now studied its interaction with purely lipidic membranes, i.e., unilamellar vesicles and planar bilayers.

EXPERIMENTAL PROCEDURES

Materials

Stichodactyla helianthus sticholysin I, called St-I, was purified and assayed as described (Alvarez et al., 1994, 1996). Egg sphingomyelin, egg phosphatidylethanolamine, egg phosphatidylcholine, and palmitoyloleoylphosphatidylcholine were all purchased from Avanti Polar Lipids and were more than 99% pure by TLC. Calcein was obtained through Sigma Chemical Co.; SDS from Pierce, Triton X-100 from Merck, and Sephadex-G50 (medium) from Pharmacia. Bovine RBC were prepared from fresh bovine blood obtained from a local slaughtery.

Methods

Preparation of Lipid Vesicles. Large unilamellar lipid vesicles (LUV) were prepared by extruding a solution of multilamellar liposomes prepared in the presence of 80 mM calcein (pH 7.0) and subjected to 5 or 6 cycles of freezing and thawing (Hope et al., 1985; MacDonald et al., 1991). A two-syringe extruder was used (LiposoFast Basic unit from Avestin Inc., Ottawa, Canada), equipped with two stacked polycarbonate filters bearing holes with an average diameter of 100 nm (purchased from Nuclepore). Thirty-one passages were performed each time. Lipids used were PC and SM at different molar ratios (as reported in the text). The starting lipid concentration was 10 mg/mL. To remove untrapped calcein, the vesicles were spun through minicolumns (Pierce) loaded with Sephadex G50 (medium) preequilibrated with 100 mM NaCl, 0.1 mg/mL BSA, 1 mM EDTA, and 10 mM Bistris, pH 7.5 [as described by Lelkes (1984)].

After gel filtration, lipid concentrations were redetermined with the Menagent phospholipid assay (Menarini Diagnostics, Florence, Italy), as described by the manufacturer with the following changes: we dispensed only 250 μL of reagent solution in a 96-well microplate instead of 2 mL in the usual 1-cm path length cuvette; the plate was read at 500 nm with an absorbance microplate reader (UVmax, Molecular Devices). This method quantitates choline groups via an enzymatic reaction leading to a colored product (Takayama et al., 1977). By using appropriate standards we ensured that the method is equally sensitive to PC and SM and that, using 50 μL of lipid solution, it gives reproducible and accurate results down to a concentration of 2 μg/mL of these phospholipids.

LUV size was determined by photon correlation spectroscopy [as in Mayer et al. (1986)] using a laser particle sizer (Malvern Z-sizer 3). We measured an average diameter of 90 ± 10 nm.

Permeabilization Assay. Permeabilization was determined by measuring the fluorescence of calcein released from the vesicles [as in Kayalar et al. (1986)], using a fluorescence microplate reader (Fluostar from SLT, Austria). Fluorescence was induced by exciting at 485 nm through a narrowband interference filter and was detected after a second filter centered at 538 nm. A black plastic 96-well microplate (Labsystems Fluoroplate) was used, filled with 400 μL of the elution buffer (with pH adjusted either to 7.5 or 8, as specified in the text) plus the desired amount of LUV. The final lipid and toxin concentrations were variable and are reported in the text. The experiments were run at room temperature. In the experiments with variable pH, the composition of the solution was the same as the elution buffer except that Bistris was substituted either by 10 mM citric acid (for pH 4 and 5), or by 10 mM Hepes (for pH 8) or by 10 mM Caps (for pH values between 9 and 11). After mixing of the vesicles with the toxin, the release of calcein from the vesicles produced an increase in the fluorescence F (due to the dequenching of the dye into the external medium) which was resolved in time. Each value reported is the average of five consecutive readings of the same well (taken in 0.5 s). Spontaneous leakage of calcein was negligible under these conditions. In some cases fluorescence was measured in a conventional spectrofluorometer (Jasco FP-550) using a 1-cm semimicro quartz cuvette containing 1 mL of buffer continuously stirred. In these experiments, excitation was set at 494 nm and emission at 520 nm. Maximum release was always obtained by adding 1 mM Triton X-100 (final concentration) and provided the fluorescence value F_{max}. The percentage of release, $R_\%$, was calculated as follows:

$$R_\% = (F_{fin} - F_{in})/(F_{max} - F_{in}) \times 100 \qquad (1)$$

where F_{in} and F_{fin} represent the initial and the final (steady-state) value of fluorescence before and after toxin addition, respectively.

In control experiments, permeabilization of small unilamellar vesicles was also determined. These were prepared as above except that in place of the extrusion step they were thoroughly sonicated as described earlier (Menestrina, 1988).

Toxin Binding to Lipid Vesicles. Binding of St-I to LUV was made evident by polyacrylamide gel electrophoresis. Calcein-loaded LUV of different composition, at a total lipid concentration between 0.03 and 0.3 mg/mL, were incubated with toxin (20 μg/mL) for 30 min at room temperature. The buffer used was the same as the corresponding kinetic experiments, except that here BSA was omitted. After the incubation the amount of calcein released was determined as above, and then the LUV with the bound toxin were pelleted by 15 h of centrifugation at 200000g in a Sorvall ultracentrifuge equipped with a swing-out rotor (TH-641) refrigerated to 4 °C.

The precipitates were collected, lyophilized, and resuspended in a volume of distilled water that would provide a protein concentration of 0.3 mg/mL if all the toxin was coprecipitated with the vesicles. A portion of this solution was mixed with an equal volume of 2.5% SDS and subjected

to PAGE as described below. Control experiments have shown that, even at a toxin to vesicle (*T/V*) molar ratio of 2000, St-I does not lyse the vesicles via a detergentlike effect as we observed, for example, with melittin (albeit at a *T/V* > 20000). Using the lipid determination method, we found that for *T/V* ranging from 2000 to 100, lipid recovery in the pellet was between 87% and 90% of that in a control tube with the same lipid concentration but no toxin. Control tubes, containing the protein but no vesicles, indicated that St-I alone does not precipitate under these conditions.

Rate of Binding. To estimate the velocity of binding, St-I, at a concentration of 92 ng/mL, was added to a solution containing different amounts of SM/PC LUV (1:1 molar ratio). After a variable delay (1, 2, 4, 8, 16, and 32 s), bovine RBC were added and the residual hemolytic activity was determined by measuring turbidometrically the rate of hemolysis (Pederzolli et al., 1995; Alvarez et al., 1996). Experiments were run in the usual buffer (0.1 M NaCl, 20 mM Bistris, 1 mM EDTA, and 0.1 mg/mL BSA, pH 7.5). By comparison with a titration of toxin alone, the amount of St-I remaining free in the solution at each moment was determined. The time course was fitted to a single-exponential decay, which provided both the rate constant and the percentage of free toxin in solution at steady state.

Polyacrylamide Gel Electrophoresis. Denaturing gel electrophoresis was performed according to Laemmli (1970) using precast gradient minigels (Pharmacia, Uppsala, Sweden) with density ranging from 8% to 25%. A semiautomatic unit, PhastSystem by Pharmacia, was employed. The run was performed with a buffer containing 0.2 M tricine, 0.2 M Tris, and 0.55% SDS, pH 7.5, at 10 °C. All protein samples were made 1.3% in SDS before being run on the gel. Gels were stained with Coomassie brilliant blue, destained, and thereafter stained again with silver. The amount of protein present in each band was quantitated by bidimensional densitometry using a PhastImage densitometer (Pharmacia), with a band-pass filter at 546 nm. The relative toxin concentration was obtained as the ratio of the optical volume of the corresponding band, measured in OD· mm², to that of the control. Linearity in this range was established through a calibration curve with free toxin.

Conductance Experiments in Planar Lipid Bilayers. Planar lipid membranes (PLM) were prepared as described earlier (Menestrina, 1986) by apposing two lipid monolayers on a 0.2-mm hole in a thin Teflon septum separating two buffered salt solutions. The monolayers were spread using different lipid mixtures, either POPC:PE 1:1 or POPC:PE:SM 1:1:0.1, as detailed in the text. The lipids were dissolved at 6 mg/mL in 49:1 *n*-hexane:ethanol. St-I was added to the *cis* compartment of a preformed stable bilayer and the current flowing through the membrane, under voltage clamp conditions, was passed through an *I−V* converter (a virtual grounded Burr Brown OPA 104C operational amplifier). The *cis* compartment was connected to the virtual ground and voltage signs refer to it; current is defined positive when cations flow into this compartment. Baseline conductance of the membranes did not exceed 50 pS. Ag−AgCl electrodes were used. Bathing solutions, 4 mL of 0.1 M KCl and 10 mM Hepes, pH 7.0, on each side, were stirred and kept at room temperature. For the selectivity experiments the solutions contained 1 mM EDTA and 30 mM Tris (pH 7.0) plus 20 or 200 mM NaCl in the *cis* and *trans*
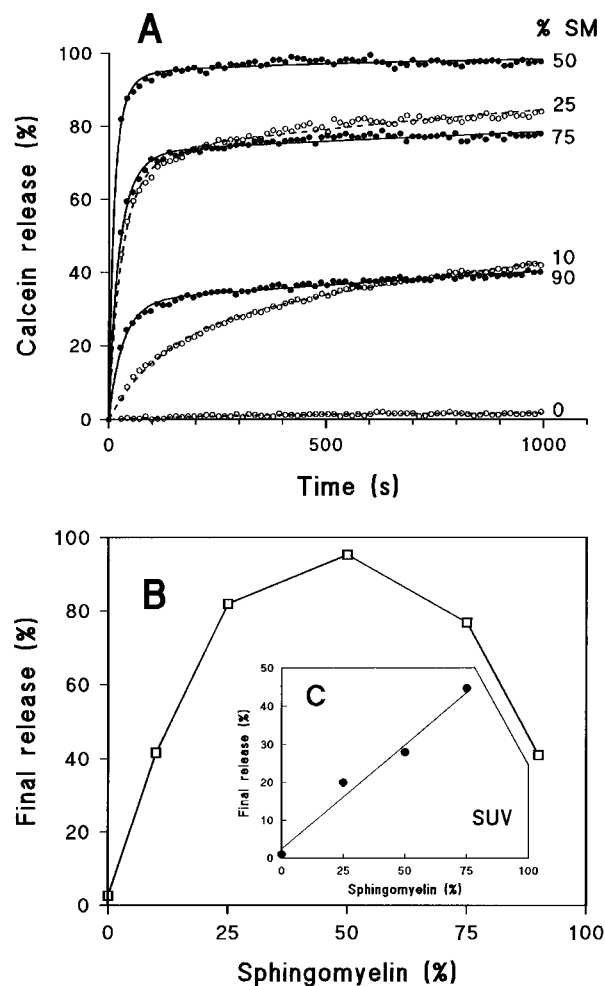

FIGURE 1: Permeabilization of LUV by St-I measured by the release of calcein. (A) Fluorescence increase after the addition, at time 0, of 0.215 μg/mL St-I to a solution with calcein-loaded LUV, measured with a microplate reader and converted to a percentage of the maximal release obtained with 1 mM Triton X-100. Only the first 1000 s are shown out of a 45-min experiment. The errors in these traces are of statistical origin, i.e. proportional to the square root of the signal, the coefficient being here 0.1. The LUV were composed of different mixtures of PC and SM; the percentage of SM present is indicated next to each trace. Lipid concentration was 3 μg/mL in all cases. Taking into consideration the size of the vesicles used, the toxin to vesicle ratio was ≈232. Lines drawn through the points are best fit according to eqs 3 and 15. The external solution was 100 mM NaCl, 0.1 mg/mL BSA, 1 mM EDTA, and 10 mM Bistris, pH 8. (B) Effect of the SM content of the LUV on the steady-state permeabilization by St-I. Final release was determined after 45 min. (C) Similar experiments except that SUV were used.

compartment, respectively. The electrodes were connected through agar bridges saturated with 1 M NaCl.

RESULTS

Permeabilization of Unilamellar Lipid Vesicles by St-I. Addition of St-I to a solution containing calcein-loaded large unilamellar vesicles demonstrated that this toxin promotes the release of the dye, as indicated by an increase in fluorescence (Figure 1A). This is consistent with the previous observation that St-I induces lysis of red blood cells by forming channels with an apparent radius of about 1 nm (Alvarez et al., 1996), which is large enough to let calcein through.

The time course and the extent of the interaction between toxin and vesicles was determined as a function of the lipid

composition. Maximal release was when SM and PC were equimolar (Figure 1B), whereas the activity with pure PC, or pure SM (not shown), was extremely low. Interestingly, at high SM concentrations, the initial rate of the permeabilization did not decrease as much as the amplitude. This is evident when one compares the traces obtained with 10% and 90% SM in Figure 1. They have a similar extent of permeabilization (very much reduced in comparison to the case of 50% SM), but a very different initial rate of permeabilization, much faster in the case of 90% SM. This behavior is somehow different from that previously reported for the action of another actinoporin, equinatoxin II (EqT-II), on SUV. In that case the effect appeared to increase steadily with the amount of SM present (Belmonte et al., 1993). In order to ascertain the reason for this variation we performed experiments also with SUV. We found that indeed, in that case, the activity was always increasing with the amount of SM, at least until 75% (Figure 1C).

It was important to determine whether the reduced permeabilizing activity at low and high SM content was due to a deficiency in toxin binding or to a deficiency in the assembly of a functional pore from bound toxin molecules. Binding was thus directly measured by first washing away unbound toxin from vesicles that were incubated with St-I and thereafter quantitating the amount of peptide remaining associated with the lipid by densitometry of the relevant SDS−PAGE band (Figure 2A). Using calcein-loaded LUV for these experiments, we could also correlate the amount of release with the intensity of the band (Figure 2B). In this way, we could show that the lack of activity was essentially due to a lack of binding.

With LUV containing 50% SM, at a T/V molar ratio of 132, the activity of St-I was optimal around pH 8 (Figure 3). At pH $\geq$ 10 the toxin became much less potent. We also noted an increased interaction at pH 4, as previously reported for EqT-II (Belmonte et al., 1993). With a molar ratio $T/V = 38$ the pattern was similar, although the local maximum at pH 8 was lower. Furthermore, also with LUV of different composition (containing either 25% or 75% SM) we had a similar trend, while LUV of pure PC or pure SM were almost insensitive at any pH value (data not shown). Also in this case, St-I binding to LUV containing 50% SM was quantitatively determined (Figure 3B, inset). Again, it was found consistent with the amount of permeabilization. In particular, the low activity at pH 11 appears to be due to a lack of binding. Interestingly, we found that at pH 8 at least 80% of the toxin is bound to the vesicles.

Titration of the Effects of Vesicles and Toxin Dose. In the case of other sea anemone cytolysins it was proposed that they formed an oligomeric pore comprising on average 4 toxin monomers (Michaels, 1979; Varanda & Finkelstein, 1980; Belmonte et al., 1993). We addressed this question by studying the kinetic of calcein release under different T/V ratios (Figures 4 and 5).

We began exposing different amounts of vesicles to the same concentration of St-I. The quantity of calcein released increased linearly with decreasing T/V ratio as long as the T/V ratio was larger than about 100, but then it decreased (Figure 4B). The percentage of release, on the other hand, was constantly decreasing (Figure 4C). The corresponding binding experiment (inset of Figure 4B) indicated that for T/V larger than 200, the amount of toxin bound increased with the LUV concentration similarly to the quantity of
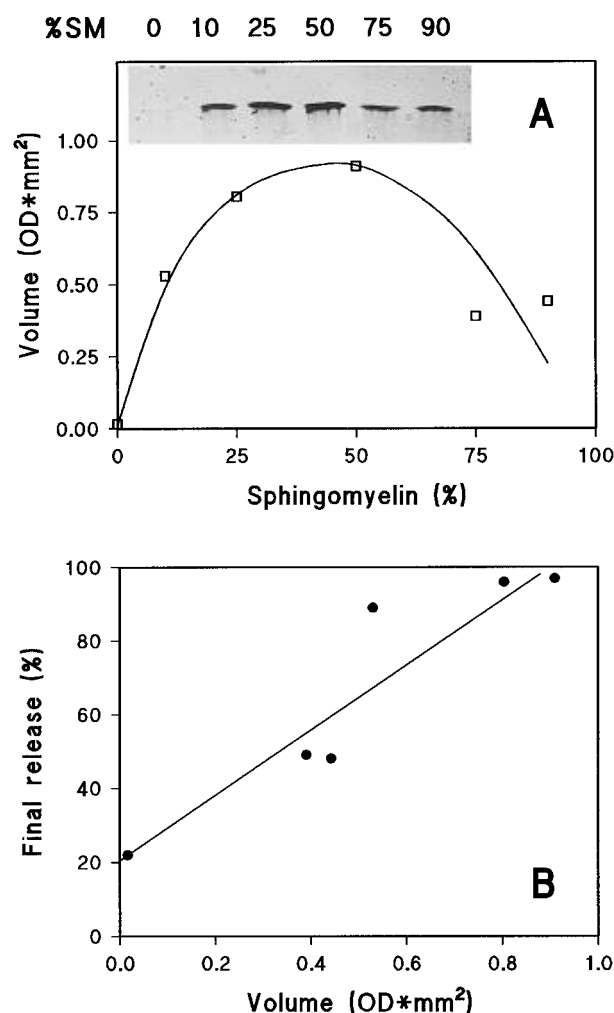

FIGURE 2: Binding of St-I to LUV. (A) LUV of different composition were incubated with toxin (20.85 μg/mL) for 30 min at room temperature. Unbound toxin was separated from the vesicles by sedimenting them via ultracentrifugation. The toxin present in the pellet (i.e., associated with the lipid) was subjected to SDS−PAGE (inset). Bands are labeled with the percentage of SM present in the LUV of that lane. The amount of toxin present in each band was quantitated by densitometry and is reported as the optical volume measured in OD·mm². Experimental error was evaluated around 15% here. Lipid concentration was 0.3 mg/mL, implying a toxin to vesicle ratio $\approx$225. Other experimental conditions are the same as in Figure 1. (B) Correlation between the extent of calcein release and the extent of binding (measured by the density of the related band) for the experiment shown in panel A. Solid line is the linear regression, correlation coefficient is $r = 0.93$; the reduced χ^2 is 1.4, which indicates that the data are well within the confidence limit.

calcein released. For T/V smaller then 200, the SDS−PAGE technique was not applicable because of the high lipid concentration necessary.

The dose dependence of the toxin permeabilization was next studied, using vesicles containing different amounts of SM (25%, 50% and 75%) at pH 8 (Figure 5). Both the rate and the extent of calcein release increased with toxin concentration (Figure 5A). A plot of the percentage of release vs toxin dose in a double-logarithmic scale (Figure 5B) had a slope larger than one for all LUV compositions. The results could be fitted to the Hill equation (Zubay, 1983), with coefficients 2.6 $\pm$ 0.4, 2.6 $\pm$ 0.6, and 2.1 $\pm$ 0.6 for vesicles containing 25%, 50%, and 75% SM, respectively. In a different set of experiments (Figure 5C) the concentration of St-I offered to a single sample of LUV was
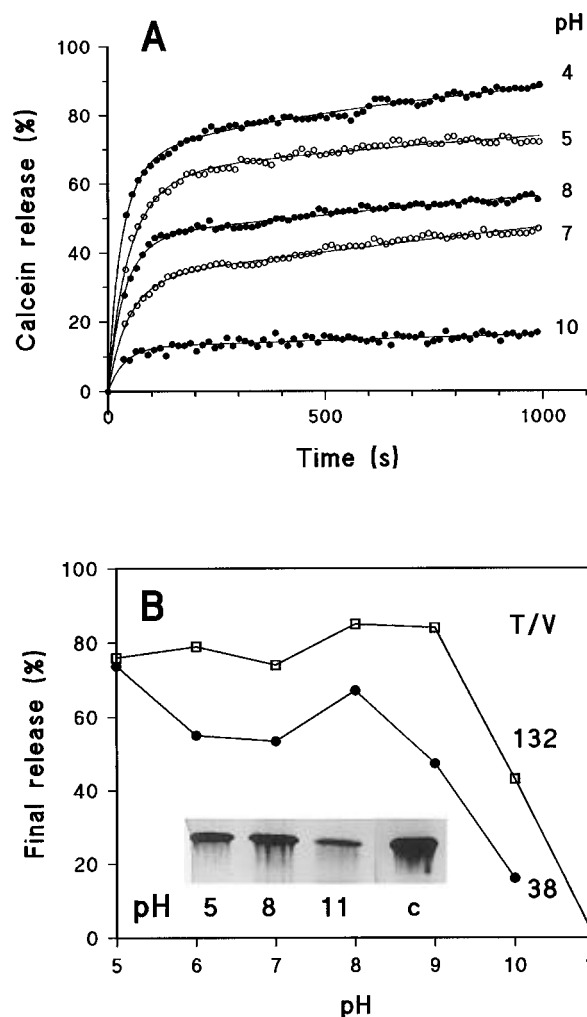
FIGURE 3: Extent of permeabilization of LUV as a function of pH. (A) Time course of calcein release, measured as in Figure 1A, after addition of 0.16 μg/mL St-I to a solution with 14 μg/mL vesicles containing 50% SM ($T/V = 38$) at the indicated pH. The experimental traces at pH 6 and 9 were omitted for clarity because they overlap the trace at pH 7. Other experimental conditions are the same as in Figure 1. Solid lines are best fit according to eqs 3 and 15. (B) Percentage of release, obtained after 45 min (as in Figure 1). Two different lipid concentrations were used, 4 and 14 μg/mL, corresponding to toxin to vesicle ratios of 132 and 38 respectively (as indicated). Other conditions were as in panel A. (Insert) Binding of St-I to the LUV was determined by ultracentrifugation and SDS−PAGE exactly as in Figure 2A, except that here the pH was varied (as indicated by the labels) while the LUV were always composed of SM/PC (1:1 molar ratio). T/V was 225. A control band (labeled c), containing the same amount of St-I that was applied to the vesicles, is also shown and provides the reference for 100% binding. The amount of St-I bound to the vesicles was estimated by densitometry to be 53%, 80%, and 16.5% for pH 5, 8, and 11, respectively. Also in this case there was a good correlation between the amount of binding and the amount of calcein released by the vesicles during the incubation (not shown).
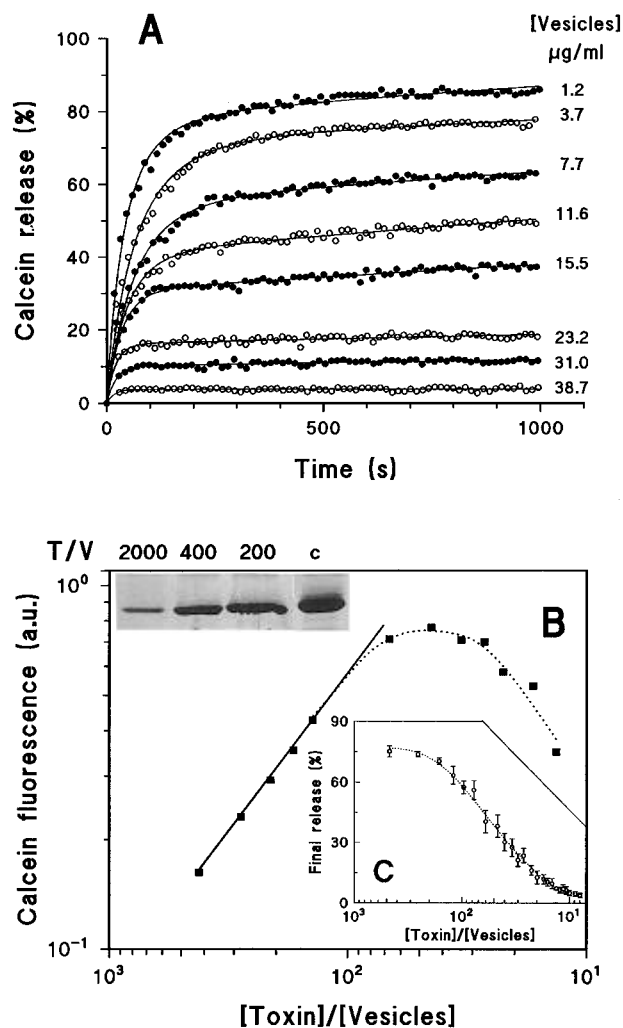
FIGURE 4: Dependence of the extent of permeabilization of LUV on the toxin to vesicles molar ratio (T/V). (A) Time course of calcein release, measured as in Figure 1A, after addition of 0.17 μg/mL St-I to a solution containing different concentrations of vesicles (as indicated). LUV contained 50% SM. Other experimental conditions are the same as in Figure 1. Solid lines are best fit according to eqs 3 and 15. The derived velocities are included in Figure 8B. (B) The amount of calcein released after 45 min (indicated by the fluorescence expressed in arbitrary units) is reported as a function of T/V. All experimental conditions are the same as in panel A. The solid line is the linear regression through the points with $T/V > 100$, providing a slope of 1; the dotted line was drawn by eye. In the inset, the binding of St-I to LUV was determined as shown in Figures 2A and 3B, except that here the LUV were always composed of SM/PC (1:1) and their concentration was varied between 29 and 290 μg/mL (corresponding to a T/V of 2000, 400, and 200 as indicated). SDS−PAGE bands, including a control band providing the reference for 100% binding (labeled c), are shown. The amount of St-I bound to the vesicles was estimated densitometrically to be 11%, 58%, and 86% for T/V of 2000, 400, and 200, respectively. The correlation between the amount of toxin bound and the amount of calcein released was good also in this case (not shown). (C) Percentage of release after 45 min for three independent experiments as in panel B. Mean $\pm$ SEM is reported; the dotted line was drawn by eye.

progressively increased by repeated additions and the percentage of release was recorded after each addition. The release increased sigmoidally with toxin concentration, indicating that LUV were not permeabilised efficiently until a critical number of monomers per vesicle was reached. Again, this was evidenced by using the Hill equation, which gave a best fit coefficient $n = 2.1 \pm 0.2$.

Formation of Ionic Channels in Planar Lipid Bilayers by St-I. Vesicle permeabilization is compatible with the forma-

tion of toxin channels into the lipid bilayer. These pores could be directly visualized using planar lipid membranes (PLM). In fact, addition of St-I to a voltage-clamped PLM, led to the appearance of stepwise increases in the conductivity of the film which were all of a similar size, implicating the formation of pores (Figure 6). In 0.1 M KCl these long-lived pores had an average conductance of around 420 pS
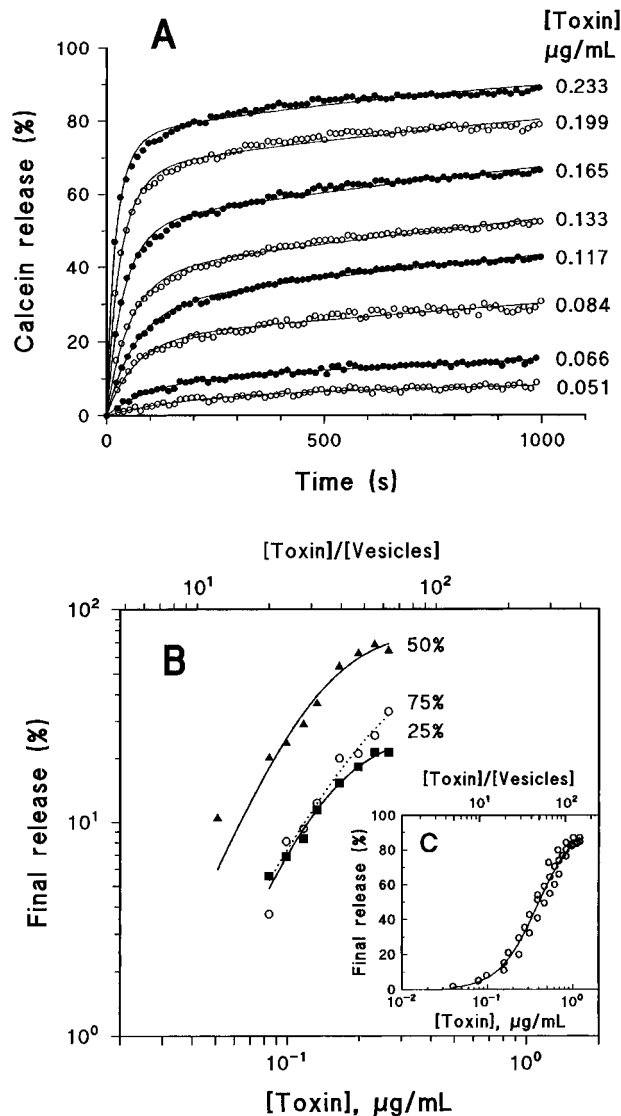
FIGURE 5: Dose dependence of the St-I-induced LUV permeabilization. (A) Time course of calcein release from SM/PC vesicles (1:1 mixture) after addition of different amounts of St-I (as indicated). Other experimental conditions are the same as in Figure 1A, except that here the lipid concentration was 14 μg/mL and the pH was 7.5. Solid lines are best fit according to eqs 3 and 15. The derived velocities are included in Figure 8A. (B) Percentage of release versus toxin concentration for LUV containing 25%, 50%, and 75% SM (as indicated). Concentration of toxin and T/V are both indicated, lower and upper scale, respectively. The lines through the points are least-squares fits of the Hill equation, providing Hill coefficients of 2.6 $\pm$ 0.4, 2.6 $\pm$ 0.6, and 2.1 $\pm$ 0.6, respectively. Other conditions are the same as in panel A. (C) Similar to panl B but a different protocol was used. Successive additions of small amounts of St-I were done to the same LUV solution (vesicles were composed of SM:PC in a molar ratio of 1:1) and the percentage of calcein released was recorded after each addition. Other conditions are the same as in panel A, except that here the lipid concentration was 27.3 μg/mL and the fluorescence was measured in a spectrofluorometer. Three independent experiments are superimposed. Solid line is a best fit of the Hill equation. Hill coefficient was 2.1 $\pm$ 0.6.

(lower panel of Figure 6). Using a transmembrane gradient of NaCl we could prove that the channel is cation-selective (Table 1): from the value of the reversal voltage we estimated that Na^+ is roughly 4 times more permeant than Cl^-.

The molecular properties of the pores formed by St-I were further investigated in relation to the applied voltage (Figure
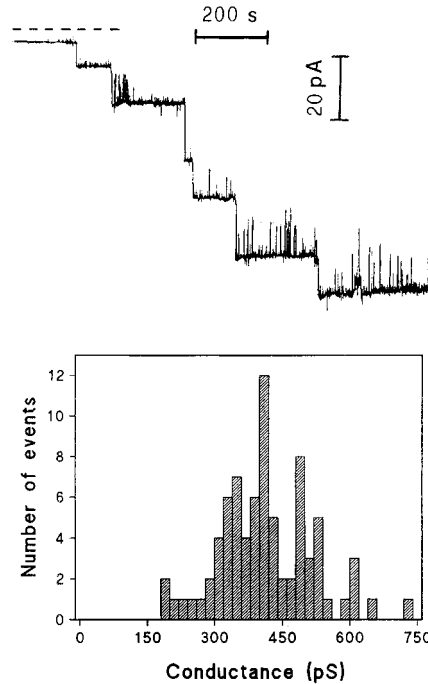

FIGURE 6: Pore formation by St-I in planar lipid membranes (PLM). Addition of St-I to one side of a PLM resulted in the opening of ionic channels which increased the conductivity of the film in discrete steps. Applied voltage was −40 mV and openings appear as downward deflections. Dashed line indicates current zero. A histogram of the distribution of the conductance of the pores observed in different experiments is reported in the lower panel. Seventy-nine events have been cumulated; average conductance ($\pm$SD) was 413 $\pm$ 104 pS. Experimental conditions were as follows: PLM prepared with POPC:PE:SM (1:1:0.1); St-I concentration 5 ng/ml; bathing solutions 0.1 M KCl and 10 mM Hepes, pH 7.

Table 1: Electrical Properties of St-I Channels in Planar Lipid Bilayers

G^a (pS)	$V_{rev}{}^b$ (mV)	$P_+/P_-{}^c$	r^d (nm)
413 $\pm$ 104	−27 $\pm$ 2	4 $\pm$ 1	1.0 $\pm$ 0.1

^{a} G is the channel conductance, calculated as the average $\pm$ SD of the events reported in the histogram of Figure 6. ^{b} V_{rev} is the voltage at which no current flows in an experiment in which the membrane separated two solutions containing 20 mM NaCl on the *cis* side and 200 mM NaCl on the *trans* side. ^{c} P_+ and P_- represent the permeability of the cation and the anion, respectively; the ratio P_+/P_- was calculated according to the Nernst−Planck equation, using the pertinent activity coefficients for the *cis* and *trans* solution (Hille, 1984). ^{d} r is the radius of the pore; it was calculated assuming that the channel is a perfect cylinder, 6 nm long, filled with water, where cations and anions move in a ratio 4:1 with the same mobility they have in solution (Hille, 1984).

7). The instantaneous current−voltage characteristic ($I−V$) was found to be nonlinear. In particular, the current flowing at negative voltages was larger than that flowing at positive voltages of the same value (Figure 7A). The steady-state probability of the pores to be open was also found to be voltage-dependent. Applications of long-lasting large voltage pulses caused the closure of the pores independently of the polarity applied, although positive voltages were clearly more effective (Figure 7B). Finally, the number of pores formed in the membrane was a function of the toxin dose. As in the case of LUV permeabilization, such dependence could be fitted to the Hill equation, giving a coefficient of 2.6 $\pm$ 0.5, indicating again a cooperative mechanism (Figure 7C). Also in this system, the presence of sphingomyelin promoted
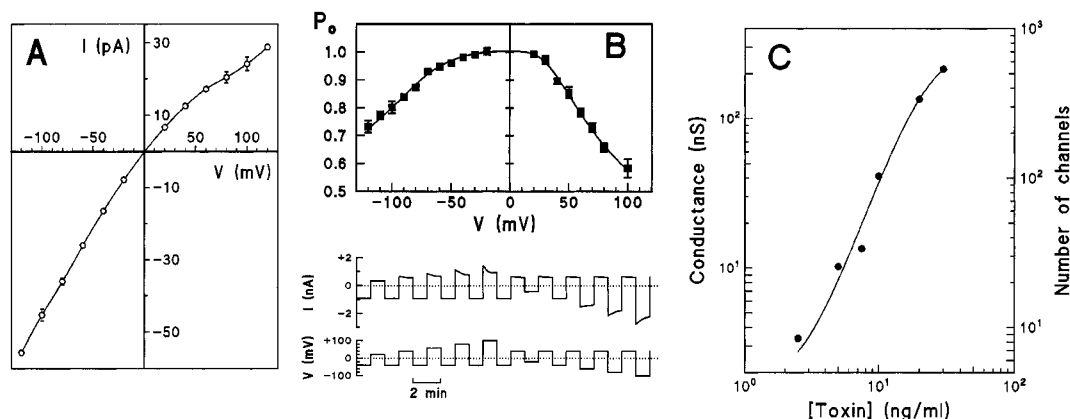
FIGURE 7: Molecular properties of the pores formed by St-I. (A) Current−voltage curves obtained applying short square-shaped voltage pulses to membranes containing many toxin channels [as described in Menestrina and Antolini (1982)]. The curve is the mean ± SD of two independent experiments scaled by dividing by the number of channels inserted in the membrane, to represent the current flowing through a single channel. Solid line was drawn by eye. PLM were prepared with POPC:PE (1:1). St-I concentration was 1 μg/mL in one experiment and 2 μg/mL in the other. Other experimental conditions were as in Figure 6. (B) Current response to the application of long-lasting square-shaped voltage pulses to membranes containing many toxin channels is shown in the lower part. For large values of potential the current declines with time after the change of voltage. For each potential, the steady-state probability P_o of the pores to be open is obtained by dividing the final stationary current by the initial value (Menestrina & Antolini, 1982). The probability curve, upper panel, is the mean ± SD of two independent experiments. Solid line was drawn by eye. Toxin concentration was 1 μg/mL. Other experimental conditions were as in panel A. (C) Dose dependence of the St-I-induced conductance in PLM. The conductance increase (left ordinate scale) of a PLM composed of POPC:PE:SM (1:1:0.1) after the addition of St-I was reported as a function of the concentration of the toxin in a double logarithmic plot. On the right scale the number of channels present is calculated using the average single channel conductance. Solid line is a best fit of the Hill equation, giving a Hill coefficient of 2.6 ± 0.5. Other conditions are the same as in panel A.

the interaction with the toxin. Typically, with SM-free membranes we had to use a 50 times larger concentration of St-I than with membranes containing 5% sphingomyelin (compare Figures 6 and 7).

DISCUSSION

All the evidence presented in this paper indicate that the sea anemone cytolysin St-I increases the permeability of model membranes by opening discrete channels. An estimate of the pore size was obtained by its conductance in PLM. Taking into account its selectivity and assuming it is simply a water-filled cylindrical channel where cations can flow as in the bulk solution, we obtained a radius of 1 nm (Table 1). This is the same size as the lesion formed in RBC (Alvarez et al., 1996), as it was estimated from the transit time of different sugars via the Renkin equation (Renkin, 1954). Nonetheless, in view of the many assumptions necessary for estimating the size either from the electrical conductance or from the Renkin equation, both these values have to be regarded as only indicative. Pore formation in PLM by a similar toxin, C-III, was described by two other groups; the conductance reported was either 350 pS in 0.1 M KCl (Varanda & Finkelstein, 1980) or 180 pS in 0.5 M KCl (Michaels, 1979). Our present results are more consistent with the first value. With EqT-II a conductance of about 200 pS was reported under similar conditions (Belmonte et al., 1993). We have indeed observed some isolated fluctuations of this size also with St-I, but only very rarely.

The instantaneous $I-V$ curve of the St-I channel is nonlinear (Figure 7A). In general this implies the existence of an asymmetrical potential profile alongside the ion pathway. This potential is most probably generated by fixed charges of the toxin which line the lumen of the pore, rendering it hydrophilic (Lindemann, 1982). A similar rectifying I/V was observed with other actinoporins, i.e., *S. helianthus* C III (Varanda & Finkelstein, 1980), *Actinia equina* EqT-II (Belmonte et al., 1993), and *Radianthus*

macrodactilus RTX (Chanturya et al., 1990). If negative, these charges could also originate the weak selectivity for cations over anions, simply by creating an electrostatic filter, as was thoroughly discussed in the case of other toxin channels (Ropele & Menestrina, 1989) or porins (Trias & Benz, 1993).

Because the toxin was effective on model membranes composed of pure lipids, it follows that a protein receptor is not strictly required for its action. It appears that sphingomyelin itself may act as an acceptor, since it strongly promotes pore formation in model membranes (Figures 1 and 2). Interestingly, with LUV, optimum activity was with 50% SM, whereas with SUV, activity always increased with SM content [see Figure 1C and previous results with *A. equina* EqT-II (Belmonte et al., 1993)]. This variation might be related to the different physical state of the phospholipids in the membrane of the LUV and the SUV. In particular, it is possible that in the SUV, which have a higher curvature, the SM headgroup remains always accessible to the toxin. In contrast, in the LUV the bilayer is practically flat and a very tight lipid packing is expected to arise at high SM content (as a matter of fact we were unable to extrude vesicles composed of pure SM). This tight packing could inhibit toxin binding and oligomerization. Because of their geometry, LUV are better models of the cell than SUV. Indeed, in the outer leaflet of mammalian cells SM is present almost in equimolar amounts with PC (together with around 50% cholesterol), thus offering the toxin the best chance to act. This finding could also explain an apparent contradiction that was reported in the course of studying the binding of *S. helianthus* C III to lipid monolayers. While the permeabilizing activity was very dependent on the presence of SM (Bernheimer & Avigad, 1976), the binding to lipid monolayers was not, being rather low either with pure PC or with pure SM (Doyle et al., 1989). Our results (Figure 1) indicate that a flat layer of pure SM is indeed a very poor target for toxin binding, just as is one of pure PC.

The most prominent pH effect, i.e. a drop of the permeabilizing activity at pH $\geq$ 10 independently of the lipid composition, might be due either to a change in the electrical charge of the toxin (the pI is 9.2) or to a conformational transition, as it was demonstrated in the case of EqT-II by studying the intrinsic tryptophan fluorescence (Macek et al., 1995). A similar pH effect was observed also for the hemolysis of rat RBC by C III (Doyle & Kem, 1989) or of sheep RBC by EqT- II (Macek & Lebez, 1981), suggesting that the events leading to vesicle and erythrocyte permeabilization are the same. In the case of pH, monolayer studies with C III gave results entirely consistent with ours; i.e., the binding increased from pH 6 to 9.5 (Doyle et al., 1989).

We addressed the problem of determining the molecularity of the St-I induced lesion by studying the effects of the T/V ratio. When we raised the lipid concentration at constant toxin concentration, the amount of vesicles permeabilized first increased linearly and then decreased (Figure 4). This excludes that the conducting pore is formed from monomers or preexisting aggregates. A linear increase followed by a constant plateau would be expected in that case. The plateau is reached when the vesicles are enough to consume all the toxin available. As pointed out for other permeabilizing peptides (Parente et al., 1990) and toxins (Forti & Menestrina, 1989), the simplest explanation for the decrease that we have observed is instead that the pore is an oligomer, formed by aggregation of monomers already incorporated into the membrane. In this case, in fact, increasing the vesicle concentration would diminish the average number of monomers incorporated per vesicle to a point that they are no longer enough to form a conducting aggregate.

This result was confirmed by the dose−response experiments (Figure 5). Under different experimental conditions we found that the permeabilization curves could be fitted by the Hill equation for cooperativity, with a coefficient between 2.1 and 2.6. Permeabilization of PLM by St-I (Figure 7) was fitted similarly with a coefficient of 2.6. This is a clear indication that toxin molecules are acting cooperatively to build up the channel. In fact, if toxin monomers (or even preformed aggregates) are the responsible for channel formation, one would expect a linear increase of the number of permeabilized vesicles up to the maximum value, providing a Hill coefficient of 1. Interestingly, fitting the dose dependence of the increase in lateral pressure of lipid monolayers exposed to *S. helianthus* C III, taken from Doyle et al. (1989), we obtained a Hill coefficient of 1.04, showing that adsorbtion is noncooperative. Aggregation, with the formation of the pore, must therefore be a later event. A Hill coefficient larger than 2 clearly suggests oligomerization but cannot provide the true molecularity of the assembly. For this, we undertook a complete theoretical analysis of the kinetic process of vesicle permeabilization. We found that it fits very well to a model introduced by Schwarz and co-workers to describe the poration of small unilamellar vesicles by melittin (Schwarz et al., 1992). This finding is not completely surprising since a strong structural similarity between the N-terminus of actinoporins and melittin was already pointed out (Belmonte et al., 1994). Although the analysis of our kinetic experiments closely follows the original (Schwarz et al., 1992), we will summarize here the basic equations of the model for the sake of clarity and for two further reasons: first, all the main assumptions of the model need to be justified for our case,

and second, some simplification that were introduced by Schwarz et al. (1992) have not been used here.

Kinetic Analysis. The basic equation of the model relates the efflux function, $E(t)$, i.e., the fraction of vesicles still intact at time t, with the average number of pores per vesicle at that time, $p(t)$, assuming a Poisson distribution (Schwarz & Robert, 1990; Schwarz et al., 1992):

$$E(t) = \exp[-p(t)] \qquad (2)$$

In our case, at each time, we measured the percentage of release, $R_\%(t)$, which is related to $E(t)$ by

$$R_\%(t) = 100[1 - E(t)] = 100[1 - \exp(-p(t)] \qquad (3)$$

These expressions are based on the assumption that one single pore is large enough to deplete a vesicle in a time comparably short with the kinetics of channel formation. In our case, we have seen that in the absence of a large transmembrane voltage the pores are open most of the time and have an average radius of 1 nm (Figures 6 and 7 and Table 1). It can be calculated that a vesicle with diameter 90 nm is depleted in less than 10 ms through a similar pore (Schwarz & Robert, 1990; Stein, 1990), i.e., much faster than all our permeabilization curves. Accordingly, such curves could be fitted to eq 3 using an appropriate expression for $p(t)$. Calculation of $p(t)$ required the development of a complete scheme for the formation of one channel. This process was divided in two steps: association of monomeric toxin with the lipid and assembly of the channel.

Scheme 1

$$c_F + c_L \underset{d}{\overset{a}{\rightleftharpoons}} c_1$$
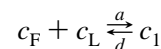
The first step is governed by Scheme 1, where c_F and c_L represent the concentration of toxin and lipid available for association, c_1 is the concentration of associated toxin, and a and d are the association and dissociation rate constants, respectively. In general c_F and c_L are different from the total concentration of toxin and lipid present, designated c_T and c_{Ltot}, respectively. However, in our kinetic experiments the lipid was always in such an excess (the ratio c_{Ltot}/c_T was constantly larger than 200) that we can safely assume that $c_L = c_{Ltot}$. It follows that

$$a/d = \Gamma = c_1/(c_F c_L) \qquad (4)$$

where Γ has the role of a partition coefficient. Introducing the molar ratio of monomeric toxin bound per lipid

$$r_1 = c_1/c_L \qquad (5)$$

we have

$$r_1 = \Gamma c_F = \Gamma c_T/(1 + \Gamma c_L) \qquad (6)$$

where the law of mass conservation was used.

As we will see later, Γ was derived from the kinetics as a fit parameter but was also directly determined from the binding experiments with a generally good agreement.

The second step to the formation of the pore is the aggregation of n toxin monomers to form a conducting unit. We found that, as in the case of melittin, the formation of a trimer is adequate to describe the kinetics. In fact we can

Table 2: Binding of St-I to Lipid Vesicles: Kinetic and Steady-State Parameters[a]

| [lipid] (μg/mL)	T/V	[toxin]$_F$ (%)	K (s^{-1})	3τ (s)
2	149.0	51.8	1.2	2.52
4	74.5	40.7	1.7	1.79
8	37.3	34.6	3.3	0.91
16	18.6	29.6	3.5	0.86
32	9.3	27.2	4.2	0.72
64	4.7	25.3	6.0	0.50

[a] St-I, 92 ng/mL, was added to a solution containing the reported amount of SM/PC (1:1) LUV. The molar ratio toxin/vesicles, T/V, is also given. The amount of toxin remaining free after a variable incubation time was determined from its hemolytic activity as detailed under Methods. The time course was fitted to a single exponential decay (average correlation coefficient $\pm$ SD was 0.996$\pm$0.003), providing the rate constant (K) and the percentage of free toxin left in solution at steady state ([toxin]$_F$). The reported time, 3τ, is the time at which 95% of the partition is accomplished.

use Scheme 2, where A_j indicates the j-meric species of the bound toxin, whose molar ratio per lipid is given by

$$r_j = c_j/c_L \tag{7}$$

with j ranging from 1 to 3, and since A_3 is the pore, $r_3 = r_P$, which is the molar ratio of pores per lipid.

Scheme 2

$$2A_1 \underset{k_{21}}{\overset{k_{12}}{\rightleftharpoons}} A_2 \overset{k_{23}}{\longrightarrow} A_3$$
$$A_1$$
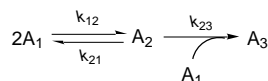
It is further assumed that the first partition step is very rapid as compared to the subsequent aggregation process and that r_1 is always in excess over the other bound species, implying that r_1 remains practically constant during the kinetics. We verified the first condition experimentally (Table 2); in fact, the partition requires at most a few seconds under a variety of lipid concentrations. The second condition, on the other hand, was consistent with our experience with a related actinoporin, EqT-II: we found that even after extensive cross-linking to stabilize toxin oligomers, monomers were always the most abundant species present on lipid vesicles (Belmonte et al., 1993).

From Scheme 2, it follows that

$$\frac{dr_2}{dt} = k_{12}r_1^2 - (k_{21} + k_{23}r_1)r_2 \tag{8}$$

and

$$\frac{dr_3}{dt} = k_{23}r_1r_2 \tag{9}$$

Using r_{2i} and r_{2f} for the initial and the final values of r_2, and with the above assumption of constant r_1, eq 8 is easily integrated to give

$$r_2 = r_{2f} + (r_{2i} - r_{2f}) \exp(-kt) \tag{10}$$

where

$$k = k_{21} + k_{23}r_1 \tag{11}$$

and

$$r_{2f} = k_{12}r_1^2/k \tag{12}$$

If we call v_P the rate of formation of pores in a vesicle we may write

$$v_P = \mu \frac{dr_p}{dt} = \mu \frac{dr_3}{dt} \tag{13}$$

where μ is the number of lipid molecules per vesicle, i.e., 81 000 as derived from the average vesicle diameter of 90 nm that we have determined by quasi-elastic light scattering.

Since

$$p(t) = \int_0^t v_p \, dt \tag{14}$$

Substitution of eqs 9−13 into eq 14 and integration yields

$$p(t) = v_f t + (v_i - v_f)[(1 - \exp(-kt))/k] \tag{15}$$

where v_i and v_f are respectively the initial and the final rate of formation of pores in a vesicle, given by

$$v_i = \mu k_{23}r_1r_{2i} \tag{16}$$

and

$$v_f = \mu k_{23}k_{12}r_1^3/k \tag{17}$$

Our release experiments were best fitted to eq 3 [with $p(t)$ given by eq 15] and produced the velocities v_i, v_f, and k reported in Figure 8. It appears that both v_i and v_f decrease with the concentration of vesicles (Figure 8B). This is a direct consequence of the oligomerization mechanism, and when only the first partition step is taken into consideration (Table 2), the rate constant actually increases with vesicle concentration, as expected for a second-order reaction.

From the dose dependence of v_i (Figure 8A), and remembering eq 6, it was evident that, as in the case of melittin, r_{2i} had the form

$$r_{2i} = K_o r_1^2 \tag{18}$$

implying the presence of a pool of dimers at the beginning of the pore formation process.

Finally, we could use eqs 11 and 16−18 to best fit the experimental velocities of Figure 8, thus estimating all the parameters involved in the process, i.e., k_{12}, k_{21}, k_{23}, K_o, and Γ (see Table 3). Using these parameters, we could test the assumption that r_1 is always in excess over the other bound species. This condition is fulfilled if $2r_2 \ll r_1$, which leads to $2K_o r_1 \ll 1$. Under the experimental conditions of Figure 8, $2K_o r_1$ varied between 0.03 and 0.18, thus satisfying the hypothesis.

From experiments like the one in Figure 8A but performed with vesicles containing 25% or 75% SM, we could derive the same parameters also for these different lipid compositions (Table 3). It appears that with both compositions the partition coefficient Γ is much smaller than with equimolar SM. Interestingly, this corresponds well to the partition coefficient determined experimentally from the binding (Figure 2A), even though the concentration of lipid and toxin were much larger in that experiment (albeit with similar T/V). A possible reason for this change of Γ has been already discussed above. It appears that with 75% SM, although

Table 3: Kinetic and Stationary Best-Fit Parameters for the Aggregation Model[a]

variable	SM (%)	k_{12} (s^{-1})	k_{21} (10^{-3}s^{-1})	k_{23} (s^{-1})	K_o (M^{-1})	Γ (10^3 M^{-1})	$\Gamma_{binding}$[e] (10^3 M^{-1})
[lipid][b]	50	0.106	3.0 ± 1.0	40 ± 10	430	26 ± 2	13
[toxin][c]	50	0.187	3.1 ± 0.1	140 ± 10	390 ± 30	25 ± 3	13
[toxin][d]	25	0.436	2.1	108 ± 20	662	3.9 ± 0.5	7.3
[toxin][d]	75	1.202	18	240 ± 30	27 900	1.9 ± 0.2	1.5

[a] The parameters k_{12}, k_{21}, k_{23}, K_o, and Γ were all derived by a best fit of eqs 11 and 16−18 to the concentration dependence of the experimental velocities determined from calcein release kinetics as in Figures 4A and 5A. [b] The variable was lipid concentration; data are shown in Figure 8B. [c] The variable was toxin concentration; data are shown in Figure 8A. [d] The variable was again toxin concentration, but vesicles were composed of a PC/SM mixture containing either 25% or 75% SM as indicated. The parameters were derived by a fit like the one in Figure 8A with exactly the same experimental conditions, except for the lipid composition (data not shown). [e] $\Gamma_{binding}$ is the experimental partition coefficient derived from the sedimentation experiment shown in Figure 2A. There, toxin and lipid concentration were 20.85 μg/mL and 300 μg/mL, respectively, for a toxin to vesicle ratio ≈225.
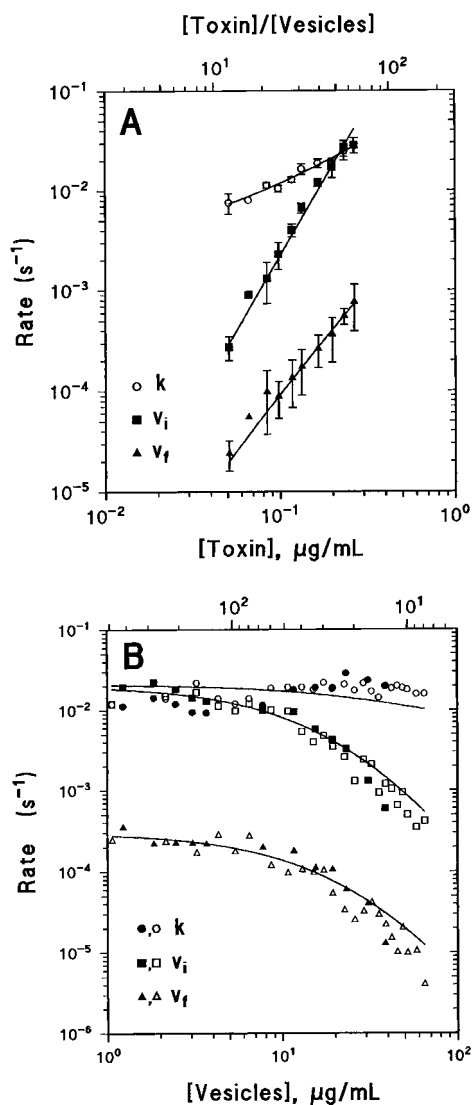

FIGURE 8: Dependence of the kinetic parameters of St-I-LUV interaction on toxin and lipid concentration. (A) The rates k, v_i, and v_f at constant lipid and variable toxin concentration were obtained by best-fitting eqs 3 and 15 to experimental traces like those in Figure 5A. They have a power dependence on toxin concentration of around 1, 3, and 2 respectively. Points are mean ± SEM of two independent experiments. Solid lines are best fits of eqs 11, 16, and 17, respectively. The equilibrium and rate constants obtained are reported in Table 3. (B) The rates k, v_i, and v_f at constant toxin and variable lipid concentration were obtained by best-fitting eqs 3 and 15 to experimental traces like those in Figure 4A. Two independent experiments were cumulated as indicated by the different symbols (open and filled). Solid lines are best fit as in panel A. The determined parameters are also reported in Table 3.

binding is lower, all the reaction rates are faster, thus accounting for the fast rise of the release with such vesicles (Figure 1A).

In conclusion, our data are consistent with the release occurring through a trimeric pore. With other actinoporins a power dependence of the permeabilizing effects on the toxin concentration between 3 and 4 was observed (Michaels, 1979; Varanda & Finkelstein, 1980; Belmonte et al., 1993), leading to the suggestion that the pore might be a tetrameric aggregate. It is possible that the pore does not have one single structure, but rather it can accommodate a variable number of monomers which come into contact by lateral diffusion into the plane of the membrane and that a trimeric pore is already able to let calcein go through. This hypothesis would be consistent with the rather broad distribution of the single-channel conductance (Figure 6). St-I failed to show stable aggregates when permeabilized vesicles were detergent-solubilized and electrophoresed in the presence of SDS (Figures 2−4). Also with EqT-II of *A. equina*, oligomers could be stabilized on vesicles only by chemical cross-linking (Belmonte et al., 1993) and, interestingly, with the same procedure toxin trimers were detected on erythrocytes (Macek et al., 1994).

REFERENCES

Alvarez, C., Tejuca, M., Morera, V., Besada, V., Pazos, I. F., Veitia, R., Luzardo, M. C., Aceved, A. M., Padron, G., & Lanio, M. E. (1994) *Adv. Mod. Biotechnol. 2*, 135.

Alvarez, C., Tejuca, M., Morera, V., Besada, V., Pazos, I. F., Lanio, M. E., Pons, T., Padron, G., Encina, M. V., Lissi, E., & Menestrina, G. (1996) *Toxicon* (in press).

Avila, A. D., de Acosta, M. C., & Lage, A. (1989) *Int. J. Cancer 43*, 926−929.

Belmonte, G., Pederzolli, C., Macek, P., & Menestrina, G. (1993) *J. Membr. Biol. 131*, 11−22.

Belmonte, G., Menestrina, G., Pederzolli, C., Krizaj, I., Gubensek, F., Turk, T., & Macek, P. (1994) *Biochim. Biophys. Acta 1192*, 197−204.

Bernheimer, A. W. (1990) in *Marine toxins: origin, structure, and molecular pharmacology* (Hall, S., & Strichartz, G., Eds.) pp 304−311, American Chemical Society, Washington, DC.

Bernheimer, A. W., & Avigad, L. S. (1976) *Proc. Natl. Acad. Sci. U.S.A. 73*, 467−471.

Blumenthal, K. M., & Kem, W. R. (1983) *J. Biol. Chem. 258*, 5574−5581.

Castañeda, O., Sotolongo, V., Amor, A. M., Stocklin, R., Anderson, A., Harvey, A. L., & Karlsson, E. (1995) *Toxicon 33*, 603−613.

Chanturya, A. N., Shaturskij, O. I., Lishko, V. K., Monastyrnaya, M. M., & Kozlowskaya, E. P. (1990) *Biol.Membr. 7*, 763−769.

Delfin, J., Gonzalez, Y., Diaz, J., & Chavez, M. (1994) *Arch. Med. Res. 25*, 199−204.

Doyle, J. W., & Kem, W. R. (1989) *Biochim. Biophys. Acta 987*, 181−186.

Doyle, J. W., Kem, W. R., & Villalonga, F. A. (1989) *Toxicon 27*, 465−471.

Forti, S., & Menestrina, G. (1989) *Eur. J. Biochem. 181*, 767−773.

Harvey, H. L. (1990) in *Handbook of toxinology* (Shier, W. T., & Mebs, D., Eds.) pp 1−66, Marcel Dekker, New York.

Hille, B. (1984) *Ionic channels of excitable membranes*, Sinauer Associates Publishers, Sunderland, MA.

Hope, M. J., Bally, M. B., Webb, G., & Cullis, P. R. (1985) *Biochim. Biophys. Acta 812*, 55−65.

Kayalar, C., & Duzgunes, N. (1986) *Biochim. Biophys. Acta 869*, 51−56.

Kem, W. R. (1988) in *The Biology of Nematocysts* (Hessinger, D. A., & Lenhoff, H. M., Eds.) pp. 375−405, Academic Press, San Diego, CA.

Laemmli, U. K. (1970) *Nature 227*, 680−685.

Lelkes, P. I. (1984) in *Liposome technology 3*: *Targeted drug delivery and biological interaction* (Gregoriadis, G., Ed.) Vol. III, pp 225−246, CRC Press, Inc., Boca Raton, FL.

Lindemann, B. (1982) *Biophys. J. 39*, 15−22.

MacDonald, R. C., MacDonald, R. I., Menco, B. P. M., Takeshita, K., Subbarao, N. K., & Hu, L. (1991) *Biochim. Biophys. Acta 1061*, 297−303.

Macek, P. (1992) *FEMS Microbiol. Immunol. 105*, 121−129.

Macek, P., & Lebez, D. (1981) *Toxicon 19*, 233−240.

Macek, P., Belmonte, G., Pederzolli, C., & Menestrina, G. (1994) *Toxicology 87*, 205−227.

Macek, P., Zecchini, M., Pederzolli, C., Dalla Serra, M., & Menestrina, G. (1995) *Eur. J. Biochem. 234*, 329−335.

Mayer, L. D., Hope, M. J., & Cullis, P. R. (1986) *Biochim. Biophys. Acta 858*, 161−168.

Mebs, D., Claus, I., Schröter, A., Takeya, H., & Iwanaga, S. (1992) in *Recent advances in toxinology research* (Gopalakrishnakone, P., & Tan, C. K., Eds.) Vol. 2, pp 392−395, National University of Singapore, Singapore.

Menestrina, G. (1986) *J. Membr. Biol. 90*, 177−190.

Menestrina, G. (1988) *FEBS Lett. 232*, 217−220.

Menestrina, G., & Antolini, R. (1982) *Biochim. Biophys. Acta 688*, 673−684.

Michaels, D. W. (1979) *Biochim. Biophys. Acta 555*, 67−78.

Parente, R. A., Nir, S., & Szoka, F. C., Jr. (1990) *Biochemistry 29*, 8720−8728.

Pazos, I. F., Alvarez, C., Rodeiro, I., & Lanio, M. E. (1996) *Biologia* (in press).

Pederzolli, C., Belmonte, G., Dalla Serra, M., Macek, P., & Menestrina, G. (1995) *Bioconjugate Chem. 6*, 166−173.

Renkin, E. M. (1954) *J. Gen. Physiol. 38*, 225−243.

Ropele, M., & Menestrina, G. (1989) *Biochim. Biophys. Acta 985*, 9−18.

Schwarz, G., & Robert, C. H. (1990) *Biophys. J. 58*, 577−583.

Schwarz, G., Zong, R.-t, & Popescu, T. (1992) *Biochim. Biophys. Acta 1110*, 97−104.

Simpson, R. J., Reid, G. E., Moritz, R. L., Morton, C., & Norton, R. S. (1990) *Eur. J. Biochem. 190*, 319−328.

Stein, W. D. (1990) *Channels, carriers and pumps. An introduction to membrane transport*, Academic Press Inc., San Diego.

Takayama, M., Itoh, S., Nagasaki, T., & Tanimizu, I. (1977) *Clin. Chim. Acta 79*, 93−98.

Trias, J., & Benz, R. (1993) *J. Biol. Chem. 268*, 6234−6240.

Turk, T. (1991) *J. Toxicol.-Toxin Rev. 10*, 223−262.

Varanda, A., & Finkelstein, A. (1980) *J. Membr. Biol. 55*, 203−211.

Zorec, R., Tester, M., Macek, P., & Mason, W. T. (1990) *J. Membr. Biol. 118*, 243−249.

Zubay, G. (1983) *Biochemistry*, Addison-Wesley Publishing Co., Reading, MA.